Molecular Crystals and Liquid Crystals Science and Technology. Section A. Molecular Crystals and Liquid Crystals

Publication details, including instructions for authors and subscription information:
http://www.tandfonline.com/loi/gmcl19

Droplet density, droplet size, and wavelength effects in PDLC light scattering

Paul S. Drzaic [a]

[a] Raychem Corporation, 300 Constitution Drive, Menlo Park, CA, 94025-1164, USA

Version of record first published: 23 Sep 2006.

To cite this article: Paul S. Drzaic (1995): Droplet density, droplet size, and wavelength effects in PDLC light scattering, Molecular Crystals and Liquid Crystals Science and Technology. Section A. Molecular Crystals and Liquid Crystals, 261:1, 383-392

To link to this article: http://dx.doi.org/10.1080/10587259508033483

Mol. Cryst. Liq. Cryst. 1995, Vol. 261, pp. 383–392
Reprints available directly from the publisher
Photocopying permitted by license only

Droplet density, droplet size, and wavelength effects in PDLC light scattering

Paul S. Drzaic
Raychem Corporation, 300 Constitution Drive, Menlo Park CA 94025-1164 USA

Abstract

The transmission properties of several scattering-type PDLC films are studied as a function of droplet density, droplet size, wavelength, and applied field. Experimental scattering cross sections for the nematic droplets are compared to theoretical cross sections calculated using the anomalous diffraction model for light scattering. Good agreement between experiment and theory is found. At low fields the scattering cross section is independent of droplet density, while at high fields the scattering cross section increases dramatically with decreasing density. These results are also rationalized using the anomalous diffraction approximation. Some implications regarding PDLC devices are discussed.

Introduction

The light scattering properties of polymer dispersed liquid crystal (PDLC) films are interesting for both scientific and technological reasons. There is an intrinsic challenge in modeling the scattering cross section of small birefringent objects, a complex and unsolved problem. The technological applications of PDLC films as electrically-controllable light shutters also provides impetus to understand the light scattering properties of these devices. The many possible variations in PDLC films (nematic properties, film morphology, droplet configuration, *etc.*) provide a rich area for study and application.

In this study I examine the scattering properties of several supramicron PDLC films. Transmission through a PDLC film is measured as a function of wavelength, liquid crystal birefringence, nematic droplet size, and nematic volume loading within the film. To model the light scattering I use a form of the anomalous diffraction (AD) approximation which has been developed to explain the light scattering of isolated, uniformly-oriented nematic droplets.[1,2] I report the novel result that in PDLC films at high fields the effective scattering cross section for droplets *increases* with *decreasing* droplet density, a result not anticipated in the isolated sphere model. Finally, I describe how the relationships established here can be used to optimize scattering properties in

PDLC-based devices: the minimization of "red-bleedthrough" at low fields and achieving the maximum clarity possible in films at high fields.

Experimental

The PDLC films were constructed by an emulsification method[3] using polyvinyl alcohol (PVA) as the film-forming polymer. PVA (Vinol 205) was obtained from Air Products; liquid crystal was obtained from E. Merck. The nematic size distribution of each emulsion was characterized using a CoulterCounter (Coulter Industries). The liquid crystal and mean volume-weighted droplet diameter (MVD) consisted of ZLI 3219 @ 2.2 μm MVD, BL003 @ 2.8 μm MVD, ZLI 1840 @ 3.1 μm MVD, and ZLI 1840 @ 2.1 μm MVD. While the mean volume-weighted diameter for the emulsions varied, the width of each distribution was nearly identical, as reported previously.[4] Emulsions with a LC:PVA ratio of 4:1 were diluted with additional PVA solutions to create emulsions with 1:4 LC:PVA ratios; this guaranteed that the droplet sizes were unchanged with dilution. Film thicknesses were measured interferometrically, while the shape of the droplets were determined through examination of electron micrographs of film cross sections prepared by a film fracture method.

The wavelength-dependent refractive indices for the liquid crystals and PVA matrix have been reported previously.[5] In the PVA matrix the solubility of the nematic is nearly zero, so that the refractive indices of the neat materials are nearly the same as those in the film. Transmission through PDLC films was measured at normal incidence with a broad-band light source equipped with ±10 nm band-pass filters centered at 450 nm, 550 nm, and 650 nm. Collection optics were $f/12$ (±2.5° acceptance angle) and transmission was corrected for specular reflection using a film blank. For the high-field measurements films were powered at 10 V/μm to insure that the nematic was well-oriented with the field.

Film structure and the AD approximation

An exact relationship between the microscopic film properties and the macroscopic film turbidity is not available at this time. Nevertheless, it is possible to apply various simplifying assumptions to make the problem tractable. The anomalous diffraction approximation is one such simplifying theory.[1,2] In the AD approximation it is assumed that light is not refracted nor reflected by passing through the nematic droplet, but undergoes only a shift in phase relative to light not passing through the droplet. The AD approximation is appropriate for PDLC films when the relationships $kR >> 1$ and $n_{LC}/n_m - 1 << 1$ hold. Here, k is the wavevector of light, R is the droplet radius, n_{LC} is

the appropriate refractive index of the liquid crystal, and n_m is the refractive index of the surrounding matrix. The films in this study at both zero field and high fields fall into the range where the AD approximation is expected to be useful.

Žumer has derived formulas for nematic droplets containing different internal configurations: a uniformly-oriented nematic structure (no internal curvature), a radial structure, and an isotropic droplet with a nematic boundary layer.[1] Afonin and Nazvanov have also proposed an expression for bipolar droplets which accounts for internal curvature within the droplet.[6] In this work I will model both the zero-field and high-field droplet scattering using the Žumer expression for a uniformly-oriented droplet structure. The difference in internal structure between a zero-field bipolar droplet and a uniformly-oriented droplet is small, and the data here shows that the uniformly-oriented expression adequately describes the scattering in both cases.

Emulsion-based films are a special case of PDLC films, as the droplets in the film possess the shape of oblate spheroids with the minor semiaxis perpendicular to the film plane.[7] This structure leads to two important factors which must be accounted for in PDLC films. First, the symmetry axis of the bipolar droplets at zero field lie in the film plane, although the azimuthal orientation varies randomly from droplet to droplet. The symmetry axes of all droplets lie perpendicular to the propagation direction of the incident light in this experiment. At high fields the droplets' symmetry axes lie perpendicular to the film plane and parallel to the incident light. Secondly, the oblate shape of the droplets means that the dimension of the droplets along the propagation direction of the incident light direction will be reduced somewhat from the diameter of the droplet in the emulsion, as measured by the CoulterCounter. This reduced dimension is important as it reduces the extent of the phase shifts which are the integral aspect of the AD approximation. Examination[4] of film cross sections by electron microscopy shows that in these emulsion-based films the average droplet has an aspect ratio of around 1.6. From this value it follows that an average droplet in the film will have a vertical dimension of $0.73*D$, where D is the MVD as measured by the CoulterCounter.

Analysis of transmission data

Equation (1) shows that the transmission T for a film depends exponentially on the film thickness d and a proportionality constant (turbidity) τ. Equation (1) is valid for PDLC films in the single-scattering regime; multiple scattering causes τ to decrease at high scattering levels. Turbidity values for these films were determined by plotting $-\ln(T)$ *vs.* d using 4–10 different films and assuming that the data lie on a straight line that passed through the origin (which it must). Other work has also shown that plots of $-\ln(T)$ vs. d are linear for thin PDLC films.[8] For the films in this study the single

scattering regime appears to hold for transmission values greater than 0.01. Figure 1 shows a plot of -ln(T) *vs.* d for one set of films at both 0.8 and 0.2 liquid crystal volume fraction.

$$T = \frac{I}{I_0} = exp\,(-\tau d) \tag{1}$$

The turbidity can be related to the microscopic cross section of the droplets through equation (2). Here, κ is a proportionality constant, N is the number of droplets, and $\langle\sigma_0\rangle$ is the average geometric cross section of the droplets. The terms in the second set of brackets relate to a scattering "efficiency factor" $H'(\nu)$ for droplet scattering under the AD approximation. In Equation (2) ν_e refers to light with a polarization vector oriented parallel to the droplet symmetry axis and ν_0 refers to light oriented perpendicular to the symmetry axis. α is the angle the polarization vector of the incident light makes with the symmetry axis of the bipolar droplet. For films at low fields α varies randomly between 0 and $\pi/2$ for each droplet. For films in this study scattering at low fields is dominated by the $H'(\nu_e)$ term and the $H'(\nu_0)$ term can be ignored. At high fields the angle $\alpha = \pi/2$ and only the $H'(\nu_0)$ term is important.

Equation (3) illustrates how the number of droplets N and the geometric cross section σ_0 depend on the volume fraction V of the liquid crystal and the average

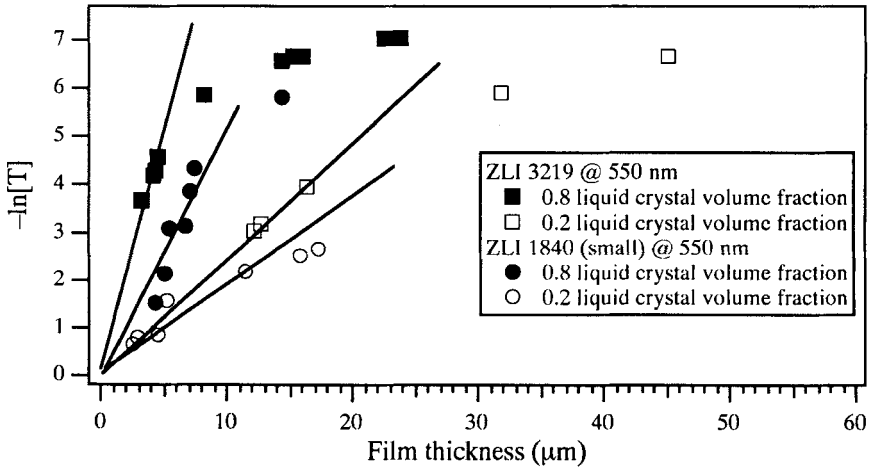

Figure 1. –ln[Transmission] vs. thickness for two of the liquid crystal systems, measured at 550 nm. The lines through the data points show the film thickness range where the single-scattering regime holds for these films. The slopes of these lines were used to determine the scattering cross section per droplet for the films.

droplet radius R. Combining Equations (2) and (3) and rearranging leads to the experimental efficiency factor H'_{expt} for each film. Here, D is the MVD and κ' is a proportionality factor. The term H'_{expt} will be compared to the theoretically-calculated values for H' calculated using the AD approximation.

$$\tau = \kappa N 2\langle\sigma_0\rangle\langle H'(\nu_e)cos^2\,\alpha + H'(\nu_o)sin^2\,\alpha\rangle \tag{2}$$

$$N\sigma_0 = \frac{V}{\left(\frac{4}{3}\right)\pi\langle R\rangle^3}\,4\pi\langle R\rangle^2 = \frac{3V}{\langle R\rangle} \tag{3}$$

$$H'_{expt} = \frac{\kappa'\tau\langle D\rangle}{V} \tag{4}$$

$$H'(\nu) = 1 - \frac{2}{\nu}sin\,(\nu) + \frac{2}{\nu^2}(1 - cos\,(\nu)) \tag{5}$$

$$\begin{Bmatrix}\nu_e\\ \nu_o\end{Bmatrix} = 2k_{air}R\left(\begin{Bmatrix}n_e\\ n_o\end{Bmatrix} - n_m\right) \tag{6}$$

Theoretical values for H' and ν defined by Equations (5) and (6), where k_{air} the wavevector of light in air, R is the radius of the droplet, n_e and n_o are the extraordinary and ordinary refractive indices, respectively, of the liquid crystal, and n_m is the refractive index of the matrix. The choice of liquid crystal refractive index n_e or n_o depends on whether the films are at zero field or high field, respectively. As described earlier, these equations are appropriate for the scattering cross section of a uniformly-aligned nematic droplet in an experiment where the light source and detector are colinear.[1,8] Equation (6) differs slightly from the original form given by Žumer as it uses the wavelength of light in air rather than the wavelength in the film.

In these experiments the experimental efficiency factor H'_{expt} and theoretical efficiency factor H' will be plotted as a function of ν. For the experimental data each the droplet size and refractive index data for each film and measurement wavelength are combined to determine an experimental value of ν. It is important to use the proper wavelength-dependent refractive index values for the liquid crystal in these calculations, as dispersion effects can cause the liquid crystal birefringence to vary by as much as 30% across the visible spectrum.[5]

Films at zero field

Figure 2 shows a plot of the experimental efficiency factors for the eight sets of films measured at three wavelengths. For the experimental data the H' terms were derived using Equation 4. The ν terms for the experimental data were obtained using Equation (6). The graph also plots the theoretical value for H' derived from the AD

approximation. It is seen that the experimental efficiency factors appear to lie on a common curve which is similar in shape to the theoretical curve. This curve shows that the scattering cross section per droplet increases until n approaches a value of 2π, when the cross section levels out. The oscillations in the theoretical curve for high values of v are not expected to be observable in these experimental data due to the broad range of droplet sizes within the film.

It is worth noting that the scattering cross section for each film appears relatively insensitive to the volume fraction of liquid crystal. The efficiency factors for 0.8 and 0.2 liquid crystal loadings differ by at most 30% across the films. As will be shown in the next section, this similarity is not the case for films at high fields.

Films at high fields

Figure 3 shows a plot of the experimental efficiency factors for the same films powered at 10 V/μm. This plot shows several differences from the plot at zero field. The most striking change is the large increase in scattering for films at 0.2 loading compared to 0.8 loading. The scattering cross section per droplet at 0.2 loading is approximately ten times larger than the cross section at 0.8 loading for all films. This difference in scattering cross section is so substantial that it is apparent in the appearance of the films to the eye. At high fields films at 0.2 loading are visibly more turbid than films at 0.8 loading and the same thickness, despite the fact that the 0.8 loading films

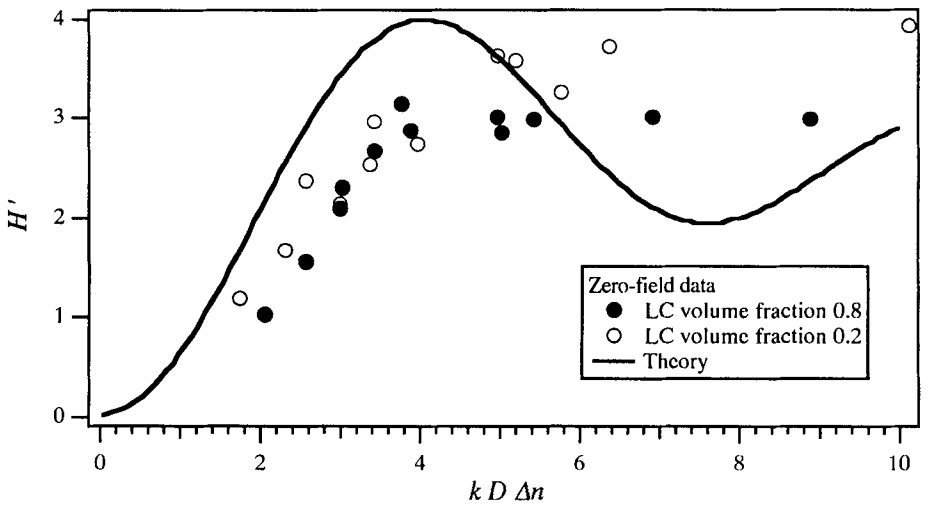

Figure 2. Scattering efficiency factor H′ for films at 0.8 and 0.2 liquid crystal volume fractions at zero field. The solid line is the calculated H' using the AD approximation.

contain four times the liquid crystal as the 0.2 loading films. This is in contrast to films at zero field, where the 0.8 volume fraction films are significantly more scattering than the films at 0.2 volume fraction (which is expected, given the similar efficiency factors and large difference in droplet density).

The agreement between the experimental and calculated efficiency factor curves is poorer at high fields (compared to the zero-field data) in these experiments. The source of this uncertainty is the relatively-large error in measuring film turbidity at high fields. At high fields all of the films in these experiments scatter light only weakly, and the measured scattering parameters are greatly affected by imperfections in the film structure that vary from film to film. These imperfections, while present at zero field also, are less obvious at zero fields since the turbidity of the films is much higher. Nevertheless, the appropriateness of the AD approximation for films at high fields has been proven in other studies where systematic experimental errors are smaller [8-11].

Scattering efficiency and droplet density

The large decrease in scattering cross section with increasing droplet density can be rationalized using the AD approximation. Recall that the basis of the AD approximation is that the scattering object within a film causes a change in the phase shift of a ray of light passing through the film. At low droplet densities, the phase shift ν of light

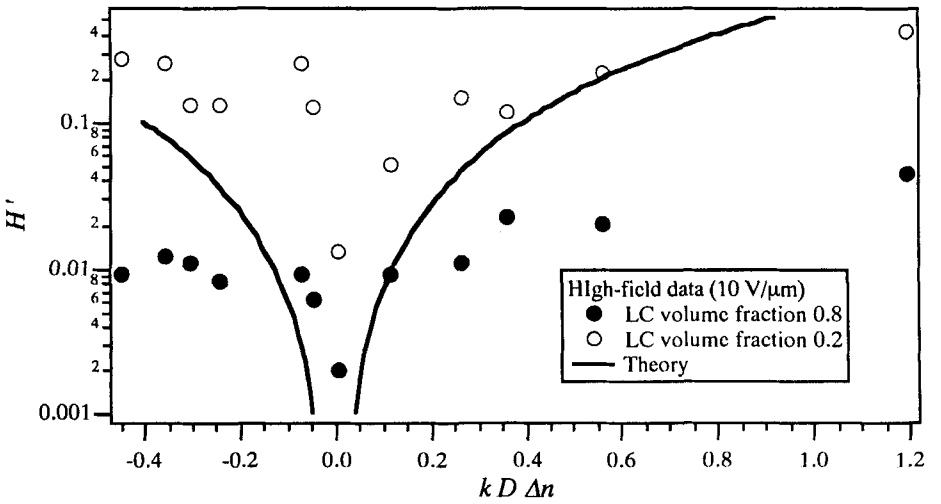

Figure 3. Scattering efficiency factor H' for films at 0.8 and 0.2 liquid crystal volume fractions at high fields. The solid line is the calculated H' using the AD approximation. The data are plotted on a log scale to show the approximate 10x difference in the efficiency factor between the films at 0.2 and at 0.8 liquid crystal loadings.

passing through a droplet (relative to the surrounding polymer) is equal to $kD(n_o-n_m)$, where D is the vertical dimension of the droplet. This phase shift determines the scattering efficiency factor of the droplet through Equations (5) and (6).

At high droplet densities, however, the film consists mainly of uniformly-oriented liquid crystal, with different domains separated by thin polymer walls (on the order of 0.2 – 0.3 μm in these films). Depending on the morphology of the film, the phase shift of light is determined by the number and thickness of the polymer interfaces that the light passes through, not the diameter of the droplet. Neighboring rays of light will be phase shifted by $kD'(n_o-n_m)$, where D′ is the thickness of one or two polymer interfaces. In a sense, the scattering objects at high loadings are not the liquid crystal droplets, but rather the polymer walls separating nematic domains.

The AD approximation predicts[1] that at low v the scattering cross section should scale as v^2. For different loadings the ratio of the relative cross sections should scale as $(D/D')^2$. An accurate calculation of the predicted cross section difference is beyond the scope of this paper, as it requires an accurate mapping of the statistical variation of droplet sizes and shapes within the films. Nevertheless, the difference between the two experimental cross sections is reasonable under the AD approximation. For the films studied here D is on the order of 2 μm (one droplet), while D' is on the order of 0.4 – .5 μm (one or two wall thicknesses). The ratio $(D/D')^2$ is then on the order of 15 – 25, which is consistent with the experimental data.

The scattering cross section of droplets at zero field is not a sensitive function of loading, unlike the high-field case. This observation can be reconciled within the AD approximation by keeping track of phase shifts. At low loadings, a ray of light can be decomposed into polarizations aligned parallel to and perpendicular to the symmetry axis of the droplet. The phase shift of the light passing through the droplet will depend on both the droplet dimension and the orientation of the droplet. Statistically, one-half the light will be strongly scattered by a droplet (seeing a large phase shift) and one-half will be only weakly scattered. The strongly scattered half will see a phase shift of $kD(n_e - n_m)$.

At high loadings each droplet is surrounded by other liquid crystal droplets, rather than polymer. The phase shift of two parallel rays passing through two adjacent droplets will depend on relative orientations of the two droplets. The refractive index of the polymer is of only secondary importance in this situation, since it's so much smaller than the droplet dimension. If the two neighboring droplets are aligned in the same direction, there is no phase shift for either polarization of one ray relative to the other. If the droplets are aligned in a perpendicular orientation, then both polarizations see a large phase shift. Statistically, one-half the light will see a phase shift of $kD(n_e - n_m)$.

In both the high and low loading cases, one-half the light will undergo a phase shift sufficiently large for strong scattering. The only significant difference in the two cases is that the phase shift depends on the difference n_e - n_m in the low-loading case and n_e - n_o in the high-loading case. For the conditions of these experiments $n_o \approx n_m$ and the phase shifts (and scattering cross sections) can be expected to be similar.

Implications for devices

For many types of PDLC devices it is important to maximize the scattering in the zero-field state and minimize the scattering in the high-field state. The correlations made in the earlier sections have important implications in the optimization of PDLC devices. The most novel result is that the clarity of films at high fields depends on the droplet density. High droplet density (and thin polymer walls) minimize the scattering in highly-oriented high-field states, while low droplet densities can lead to significant turbidity in the film.

At low fields decreasing the average droplet size usually increases film scattering. Decreasing droplet size increases the number of scattering sites within the film, and long as the scattering efficiency factor H' remains constant the total film scattering increases. However, it is well-known that light scattering becomes poor for long wavelengths of light if the average diameter for droplets in a PDLC film get too small (the familiar phenomenon of "red-bleedthrough" often seen in PDLC films).[13-14] This red-bleedthrough effect provides a practical limit to the minimum size for droplets in PDLC films where strong scattering across the visible spectrum is desired. It has been noted[14] that optimized film scattering occurs using droplets with diameters in the range of 1-10 μm for liquid crystals with birefringence values within the range of 0.05-0.26, with lower birefringence materials requiring larger droplets to avoid red-bleedthrough.

The red-bleedthrough phenomenon is related to the dependence of the scattering efficiency factor on ν seen in Figure 2. For high ν the efficiency factor depends only weakly on ν, but the scattering efficiency factor drops precipitously for low ν. As noted[1] by Žumer, this change in slope is predicted to occur when ΔnkR approaches π. From Figure 2 the data for these emulsion systems suggests that the change in slope occurs for $\Delta nkD \approx 4$ (equivalent to $\Delta nkR \approx 2$). Assigning 700 nm light as the beginning of the visible range, Figure 2 indicates that in these emulsion based films the onset for red-bleedthrough occurs when $D^*\Delta n \leq 0.45$. This relationship is consistent with the phenomenological relationship established between droplet size, birefringence, and red bleedthrough.[13-14] The difference between this experimental number and the theoretical prediction may involve the distribution of sizes and aspect ratios for droplets in the emulsion system.

For phase separation-type films red-bleedthrough is expected to occur for larger values of $R^*\Delta n$. In these films the droplet symmetry axis is randomly oriented along all three dimensions,[12] rather than two dimensions as in emulsion-based films. At zero fields this random orientation leads to a decrease in the effective refractive index (and phase shift) of light oriented along the symmetry axis. The average birefringence of a droplet will be decreased by approximately 50%. Thus, we can estimate that the onset of red-bleedthrough in phase-separation type films will occur for values of $D^*\Delta n \leq 0.9$. The limit of 0.9 may shift to lower values in films where the droplets are more spherical than the emulsion system, or where a broad distribution of sizes is not present.

Summary

The AD approximation can be used to model quantitatively the scattering cross section of supramicron PDLC films. Important parameters include the film thickness, droplet size, droplet density, liquid crystal and polymer refractive indices, and wavelength. At low fields the scattering cross section is independent of droplet density, while at high fields the scattering cross section increases with decreasing droplet density. Maximum efficiency factors for film scattering occurs in emulsion-based films with high droplet densities and $D^*\Delta n > 0.3$.

References

(1) Žumer, S. *Physical Review A* **1988**, *37*, 4006-14.
(2) van de Hulst, H. C. *Light Scattering by Small Particles*; Dover: New York, 1981.
(3) Drzaic, P. S. *Liq. Cryst.* **1988**, *3*, 1543-59.
(4) Drzaic, P. S. *SPIE Proceedings (Liquid Crystal Displays and Applications)* **1990**, *1257*, 29-36.
(5) Drzaic, P. S.; Gonzales, A. M. *Mol. Cryst. Liq. Cryst.* **1992**, *222*, 11-20.
(6) Afonin, O. A.; Nazvanov, V. F. *Sov. Phys. Tech. Phys.* **1990**, *35*, 1168-72.
(7) Drzaic, P.; Muller, A. *Liquid Crystals* **1989**, *5*, 1467-75.
(8) Whitehead, J. B.; Žumer, S.; Doane, J. W. *J. Appl. Phys.* **1993**, *73*, 1057-65.
(9) Drzaic, P. S. *SPIE Proceedings (Liquid Crystal Materials, Devices, and Applications)* **1993**, 1911, 153-159.
(10) Drzaic, P. S.; Gonzales, A. M. *Appl. Phys. Lett.* **1993**, *62*, 1332-34.
(11) Kelly, J.; Wu, W.; Palffy-Muhoray, P. *Mol. Cryst. Liq. Crystal* **1992**, *223*, 251-261.
(12) Doane, J. W.; Golemme, A.; West, J. L.; Whitehead, J. B.; Wu, B. G. *Mol. Cryst. Liq. Cryst.* **1988**, *165*, 511-32.
(13) Montgomery, G. P. Proc. SPIE **1989**, *1080*, 242-9.
(14) Van Konynenburg, P.; Wipfler, R.; Smith, J. L. Proc. SPIE **1989**, *1080*, 62-9.